Preprints of the 19th World Congress
The International Federation of Automatic Control
Cape Town, South Africa. August 24-29, 2014

An Adaptive and Online Underwater Image Processing Algorithm Implemented on Miniature Biomimetic Robotic Fish

Wei Wang * **Guangming Xie** **

* *Intelligent Control Laboratory, College of Engineering, Peking University, Beijing 100871, China (e-mail: wangweiw4y4@pku.edu.cn)*
** *Intelligent Control Laboratory, College of Engineering, Peking University, Beijing 100871, China (e-mail: xiegming@pku.edu.cn)*

Abstract: This paper proposes a novel underwater image processing approach for different targets detection and preliminary positioning of a miniature robotic fish with low computational resources. A key aspect of our approach is that the image processing algorithm is performed online, i.e., while swimming, rather than as an offline process. Another key aspect is that the algorithm distinguishes the targets adaptively within large distance range. Specifically, considering the poor quality of underwater image as well as the low computational resources of the robot, a real-time image preprocessing algorithm, named accelerated automatic color equalization(AACE) model, is first adopted to improve color contrasts and sharpness of borders of the image. Further, HSV-based adaptive threshold segmentation, lump detection, reflection elimination and landmark matching are executed successively in a robust way for locating the target and calculating the distance between the robot and target. A series of relevant experiments with the robotic fish are conducted systematically to demonstrate that the proposed image processing approach is adaptive, efficient and real-time for online applications of the vision-based miniature swimming robots.

Keywords: Underwater image processing, online and adaptive, AACE model, low computational costs, biomimetic robotic fish.

1. INTRODUCTION

As the increasing demands for underwater resources, underwater robots have been the hot research topics in the last several decades. Vision, the most direct way to acquire rich information of nearby aquatic environment, plays a vital role for underwater robots similar to the eyes for aquatic animals. For example, when executing underwater missions, such as inspection and repair of underwater man-made structures, vision-aided underwater robots can directly recognize their surrounding targets and obstacles and react timely and accurately. Therefore, underwater image processing which deals with the vision-based information of underwater robots, has draw considerable attentions within the last decades (Feihu et al. (2013); Horgan and Toal (2006); Raimondo and Silvia (2010)).

Due to the particularity of the water medium, underwater image processing is confronted with great challenge. Compared with the ground-based images, underwater images have considerably poor quality, such as marine snow, poor contrasts, color distortions and degradation. In addition, images become blurred when underwater robots are moving. Therefore, in most cases, image preprocessing is the first step to enhance the quality of underwater images. Several underwater image preprocessing algorithms have been proposed in the literature (Bazeille et al. (2006); Chambah et al. (2003); CJ and PU (2011); Iqbal et al. (2007); Mahiddine et al. (2012)), which resulted in remarkable improvements in image quality. Nevertheless, most of these algorithms process offline videos acquired by underwater instruments. Moreover, they always run on computers and take high computational costs.

Followed by image enhancement, underwater image processing is executed to extract specific information (for instance, target and obstacle) for different applications, such as station keeping and localization. Many image processing algorithms have been proposed and partially implemented on the underwater robots. Nevertheless, the majority of them are executed offline similar to the preprocessing procedure (Lee et al. (2012); Sehgal et al. (2004)). In addition, the algorithms are basically designed for underwater robots with large size and on-board PC system (Lee et al. (2012); Sehgal et al. (2004); Yu et al. (2001)). Generally, these robotic systems possess high computational ability and large energy storage, which can afford to run complex image processing algorithms to suit many underwater situations (Feihu et al. (2013)). On the other hand, as the biomimetic swimming robots with miniature size and high flexibility have draw more and more attentions in recent years, the corresponding low computational image processing algorithm is in urgent need of being developed and applied on those robots. Although several suitable algorithms have been established and applied on the miniature underwater robots (Hu et al. (2009); Negre et al. (2008)), they never mentioned the preprocessing algorithm for improving the image quality.

Therefore, based on the previous projects on vision-based robotic fish (Wang et al. (2013)), this paper proposes a novel adaptive and online underwater image processing approach for different targets detection and preliminary positioning of a miniature robotic fish with 5 Hz refreshing rate. Compared with other underwater image precessing algorithm, online, adaptive and low-computation are three main aspects of our approach. In particular, a real-time AACE algorithm is first adopted to

improve underwater image quality under the low computational costs condition. Further, HSV-based adaptive threshold segmentation, lump detection, reflection elimination and landmark matching are executed successively for locating the target and calculating the distance between the robot and target in a robust way, which can be employed for further online localization and motion control.

The rest of this paper is organized as follows. Section II proposes the AACE algorithm for underwater image preprocessing. Section III gives the description of underwater image processing. The robotic fish and experimental platform are described in Section IV. Systematical experiments and results are provided in Section V to validate the proposed approach. Section VI concludes this paper.

2. UNDERWATER IMAGE PREPROCESSING: AACE MODEL

Besides the common problems of underwater image, online image processing is confronted with image blur caused by the moving robot. Therefore, considering the enhancement of image quality as well as the low computational resources of robot, an AACE model is adopted for image preprocessing.

Inspired by some adaptation mechanisms of the human vision, ACE model is able to adapt to widely varying conditions of light intensity and to extract visual information from the environment effectively. It can improve the quality of images, mainly in controlling the color contrasts, maximizing image dynamic range and sharpening boarder of image (Artusi et al. (2006)). However, as the high computational costs of ACE, it can not be competent to real-time applications. Therefore, an accelerated ACE (AACE) model (Artusi et al. (2006)), which sharply decreases the computational time, is slightly revised and adopted in this paper. The scheme of AACE is exhibited in Fig. 1, where I_c is the input image, $I_{sub,c}$ is a subset of the original image obtained by random sampling, $R_{sub,c}$ is an intermediate result of the selected subset, $O_{sub,c}$ is final output of the selected subset, O_c is final output of the whole input image and subscript c respectively denetes R, G, B chromatic channels as the original output format of camera is RGB.

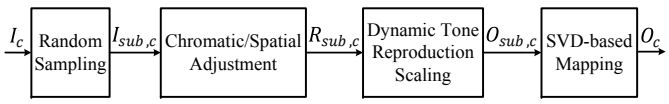

Fig. 1. The main structure of the AACE model.

To decrease the computational cost drastically, AACE first selects a subset, $I_{sub,c}$, from the original image by random sampling. Note that the size of the selected image can be used to regulate the computational time for different applications. Then, an intermediate image $R_{sub,c}$ is obtained by transforming each pixel i separately for each channel c, namely

$$R_{sub,c}(i) = \frac{\sum_{i,j\in I_{sub},j\neq i} \dfrac{r(I_{sub,c}(i) - I_{sub,c}(j))}{d(i,j)}}{\sum_{i,j\in I_{sub},j\neq i} \dfrac{r_{max}}{d(i,j)}} \tag{1}$$

where $d(i,j)$ is an Euclidean distance weighting the global and local filtering effect. The denominator is a normalization factor, which is introduced to avoid vignetting near borders of image. The term r_{max} is the maximum value of $r(\cdot)$ function, which is defined as a signum function:

$$r(\rho) = \mathrm{sgn}(\rho) = \begin{cases} -1, & \text{if } \rho < 0; \\ 0, & \text{if } \rho = 0; \\ 1, & \text{otherwise.} \end{cases} \tag{2}$$

Next, for the purpose of enhancing detail quality of the image, an additional global balance between gray world and white patch is added to extend dynamic range of R_{sub} to $[0,\ D_{max}]$. The output takes the form

$$O_{sub,c}(i) = \mathrm{round}[D_{mid} + s_c R_{sub,c}(i)] \tag{3}$$

where D_{max} is the available dynamic maximum value. For RGB format in this paper, D_{max} = 255, $D_{mid} = D_{max}/2$ and $s_c = D_{mid}/max(R_{sub,c}(i))$.

After that, polynomial functions are used to define the mapping function between the input subset $I_{sub,c}$ and the output subset $O_{sub,c}$. Here the first order polynomial is considered and defined as follows:

$$R_o = a_{11} + a_{12}R_i + a_{13}G_i + a_{14}B_i \tag{4a}$$

$$G_o = a_{21} + a_{22}R_i + a_{23}G_i + a_{24}B_i \tag{4b}$$

$$B_o = a_{31} + a_{32}R_i + a_{33}G_i + a_{34}B_i \tag{4c}$$

where index i stands for the input subset image and index o stands for the output subset image processed by AACE algorithm. The coefficients a stand for the unknown coefficients that control the behaviour of the mapping function. Generally, these polynomial functions are over-determined system. Hence, SVD method is used to extract these unknown coefficients. Once behaviours of the mapping function are extracted, they are applied to the whole input image I_c to acquire the final output image O_c .

3. UNDERWATER IMAGE PROCESSING

After preprocessing, the image quality improves quite a few. Nevertheless, problems of image noises, image reflections and color distortions are still existing in the images. These problems are tackled by using an adaptive as well as efficient image processing strategy, which is mainly illustrated in Fig. 2. Finally, the distance between the robot and the target is obtained online in an adaptive and efficient way.

3.1 HSV-based Adaptive Threshold Segmentation

First, HSV (Hue, Saturation and Value) color space is employed for threshold segmentation. It is basically different from the well-known RGB color space since it separates out the intensity (luminance) from the color information (Sural et al. (2002)). Thus, it can avoid the effect of nonuniform illumination in underwater environment to a great extent. Furthermore, we find that the color contracts between the target and background gradually get higher as the distance (d_s, explicitly defined in later section) between the robot and target get closer. Therefore, we make use of d_s to regulate color threshold of the target adaptively, which results in robust target color extraction.

We experimentally choose Hue chance as the dominant feature to identify colors of the targets. First, the AACE-processed

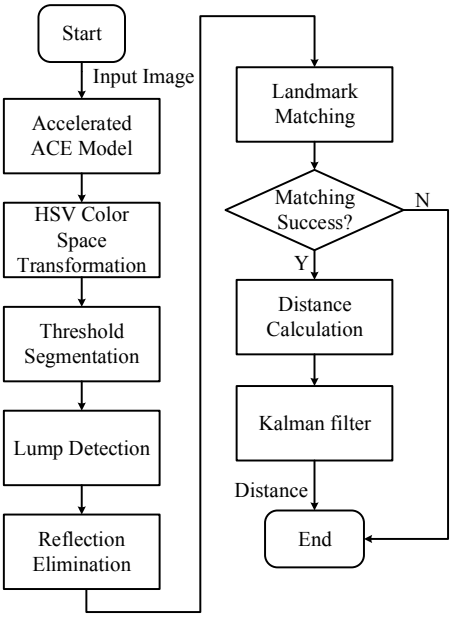

Fig. 2. Flow diagram of online underwater image processing algorithm.

image O_c is converted from RGB color space to HSV color space. And from now on, the subscript c will respectively denote H, S, V channels. Then, each pixel i will be recognized adaptively as color v, if it satisfies

$$\begin{cases} \mathrm{H}_v^{\min} - k_v d_s < O_h(i) < \mathrm{H}_v^{\max} + k_v d_s \\ O_s(i) > \mathrm{S}_v^{\min} \\ O_v(i) > \mathrm{V}_v^{\min} \end{cases} \tag{5}$$

where v denotes red, yellow and green in this paper, k_v denotes the regulating factor of color v, $\mathrm{H}_v^{\min}$ and $\mathrm{H}_v^{\max}$ denote the lower and upper threshold of color v in Hue channel, $\mathrm{S}_v^{\min}$ and $\mathrm{V}_v^{\min}$ are minimal values for Saturation and Value channels, respectively. $\mathrm{S}_v^{\min}$ and $\mathrm{V}_v^{\min}$ are applied to get rid of the noises in image background. Thresholds of target colors are obtained by plenties of experiments in advance.

3.2 Lump detection and Reflection Elimination

After adaptive threshold segmentation, both targets and some noises are extracted at the same time. In most cases, the targets gather lumped while the noises are single or in small groups, hence, a lump detector is introduced to dispose of the noises. The detector has a lump window (i. e., critical size) to judge the obtained lumps: while the size is larger than the critical, the corresponding lump is recorded, otherwise, the lump will be removed.

Next, since the underwater target is close to the surface of the water, there is a reflected lump in the image. In addition, noises sometimes are also mistakenly detected as lumps. Considering that the real lump is always the maximum and takes lower position, one simple reflection elimination approach is presented, as illustrated in Fig. 3. Note that when more than two lumps are detected, the real lump is generated by voting.

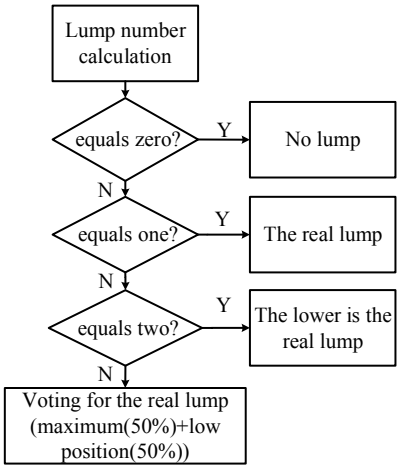

Fig. 3. Flow diagram of reflection elimination.

3.3 Landmark Matching and Distance Calculation

After reflection elimination, landmark matching is performed to identify the real target. To improve the robustness of recognition, we use two different colored landmarks parallel linked as an effective target. First, an open-source contour approximation function (in OpenCV library) is used to independently extract the rectangular profile of the two colored landmarks. Then, the target matching succeeds if the distance between central lines of two landmarks are less than a critical value, both in vertical and horizontal directions. The small critical values indicate that the two landmarks are linked with tolerated recognition errors in boundary.

Finally, when effective target is detected in the image, basically, according to pinhole imaging principle, the distance between the robot and the target is calculated. Fig. 4 shows related parameters in distance calculation and the distance d_s is defined as follows

$$d_s = \sqrt{{d_c}^2 + m^2} = \sqrt{(\frac{d_f h}{h_o})^2 + (\frac{m_o h}{h_o})^2} \tag{6}$$

where d_c is the distance between the optical center of camera and the center of field, m is the distance between the center of field and center of target, h is the height of the target, m_o is the distance between the center of field and center of landmark in the image plane, h_o is the height of the target in the image plane. d_f is the focal length of the camera which can be obtained by $d_f = d_{min} L_0 / h$ where L_0 is the height of the image plane in pixels ($L_0 = 144$ in this paper) and d_{min} is the distance between the camera and the landmark when the landmark is filled with the image plane in the longitudinal direction. And d_{min} is obtained by experimental measurement in advance. Note that unit of h_o, m_o, d_f and L_0 is pixel while unit of m, h and d_{min} is meter. We suppose that central line of the target and center of the camera are in the same horizontal plane, which is roughly satisfied with careful target arrangement. In the end, Kalman filter is adopted to smooth the calculated distance, which provides a stable output for further applications.

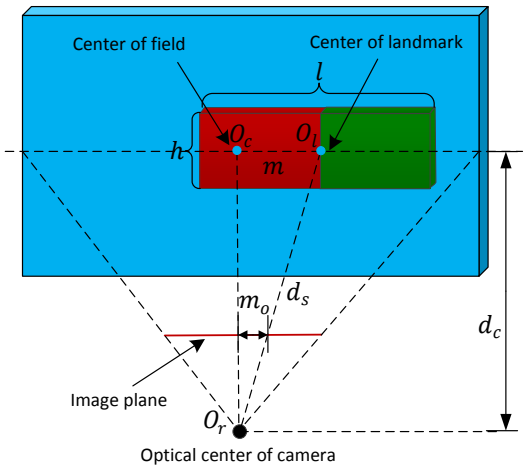

Fig. 4. Schematic diagrams of the distance and angle measurement.

4. ROBOTIC FISH AND EXPERIMENTAL PLATFORM

4.1 Overview of Robotic fish

Configuration of the autonomous/wireless-controlled robotic fish is illustrated in Fig. 5. It consists of a well-streamlined main body, a pair of pectoral fins and one caudal fin, and therefore the robot can perform multiple swimming modes, such as forward and backward swimming, turning and pitching. In particular, Raspberry Pi, a credit-card-sized and low-cost micro computer, is adopted as the main controller of the robot. It has a Broadcom BCM2835 system on a chip (SoC), which includes an ARM1176JZF-S 700 MHz processor. The robot is autonomously operated by a Linux system (Debian). Moreover, a low-cost tiny COMS camera with 1.3 million pixels is used to acquire underwater images. The maximum size of image of the camera is 1024×768 pixels. However, size of 176×144 pixels is adopted in the experiments, for the purpose of satisfying the real-time requirement with the low-performance processor.

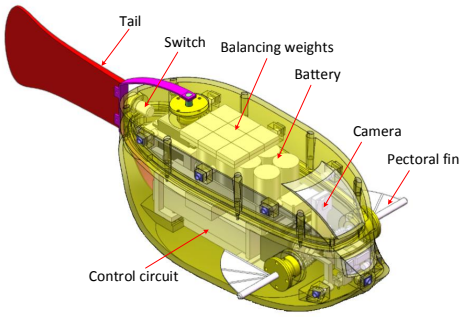

Fig. 5. The configurations of robotic fish.

4.2 Experimental Platform

In the experiments, the robot swims in a swimming tank (300 cm $\times$ 200 cm $\times$ 30 cm) with six targets (effective landmarks) uniformly distributed against the wall of tank. The targets are generated by different colored landmarks with combinations of red, yellow and green, which are RG, GR, YR, RY, GY and YG. RG and GR denote, respectively, red-green and green-red, and so on. The experimental scenario is exhibited in Fig. 6. Generally, the image processing algorithm is executed by the robot online, when the robot swims towards different targets from a distance of 150 centimeters. At the same time, the related results are recorded and restored on the flash of Raspberry Pi in real time. Simultaneously, a vision tracking platform is used to track position of the robot and calculate the distance between the robot and the target by using an overhead HD camera. The maximum errors of the tracking platform is 3 cm, therefore, the calculated distance by the tracking platform is regarded as the real distance.

Fig. 6. The swimming tank and robotic fish in the experiments.

5. EXPERIMENTS AND RESULTS

The proposed image processing algorithm is validated on a miniature robotic fish. Systematically, results of AACE preprocessing, image processing and the calculated distance are provided to show adaptiveness and high-efficiency of the online algorithm while the algorithm is running on the miniature swimming robot with low computational resources.

5.1 Results of AACE Preprocessing

This section demonstrates the contrastive results between the original and AACE-processed images, obtained while the robot is swimming to different targets, as illustrated in Fig. 7. It is obvious that the quality of images is remarkably improved after AACE preprocessing. Specifically, thep colors of AACE-processed images become more bright, borders get more sharped and the color contrasts are enhanced. These improvements deeply benefit the subsequent image processing, which will be validated in later section. Therefore, the proposed AACE algorithm gives a satisfactory solution to the poor quality of underwater image.

More importantly, the AACE algorithm takes low computational costs. This makes it a reality for image preprocessing on the miniature underwater robots with low computational resources, especially for those biomimetic swimming robots with embedded systems.

5.2 Results of Image Precessing

After preprocessing, image processing is performed in a robust way. Figure 8 shows the contrastive results of image processing while the robot catches sight of a red-green target. From Fig. 8(b) and (c), we can see that the noises have been remarkably removed after AACE. This is due to that AACE amplifies the color contrast between the target and the noises. After lump detection, small noises are completely dislodged and the possible landmarks are sought out, as exhibited in Fig.

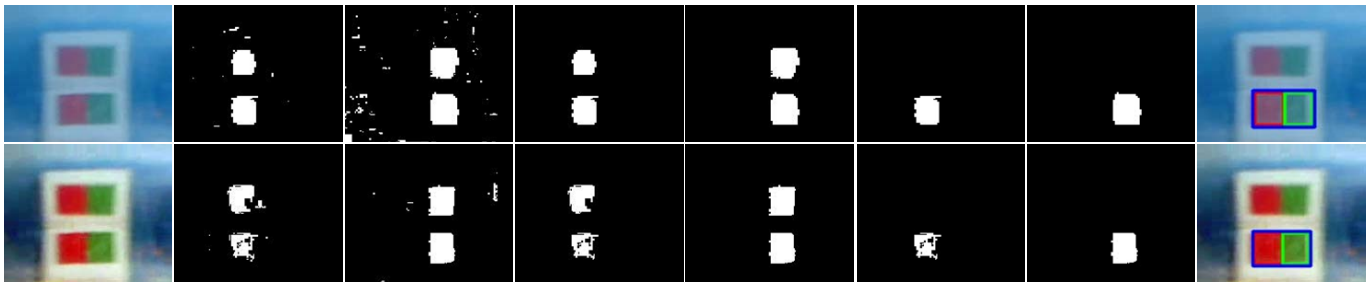

Fig. 8. Contrastive results of the image processing with (down) and without AACE (up). (a) The original images. (b) Recognized red color after threshold segmentation; (c) Recognized green color after threshold segmentation; (d) Recognized red lumps after lumps detection; (e) Recognized green lumps after lump detection; (f) Recognized red lump after reflection elimination; (g) Recognized green lump after reflection elimination; (h) Recognized final target.

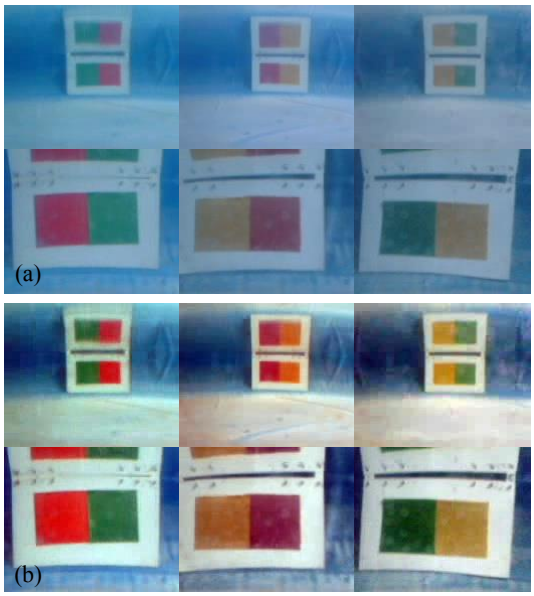

Fig. 7. Pairs of images before (a) and after AACE preprocessing (b), when robotic fish is swimming at a distance of 150 cm and 50 cm to the target.

8(d) and (e). In the pictures, the target is identified both with and without AACE. Nevertheless, a careful inspection reveals that the AACE-processed result has higher accuracy, since the recognized target without AACE has a small shift to the right direction compared with the real target. This is also verified by Fig. 8 (e) and (g).

Furthermore, the adaptiveness of the algorithm is systematically tested by massive experiments where the robot swims to different targets from the distant to the near. Figure 9 illustrates the contrastive results with and without AACE at the same time. It is obviously observed that AACE extends the robot's ability in target perception distance. In addition, AACE-processed results have a higher accuracy in the recognized size of target. This may benefit further vision-based applications, such as motion control and localization.

More commonly, recognition ratios of the algorithms are calculated. As shown in Table I, at the greater distance (120 cm $\sim$ 150 cm), AACE remarkably improves the final target recognition ratios of the robot. Broader sensing range is of great significance for the robot in an unknown environment since it

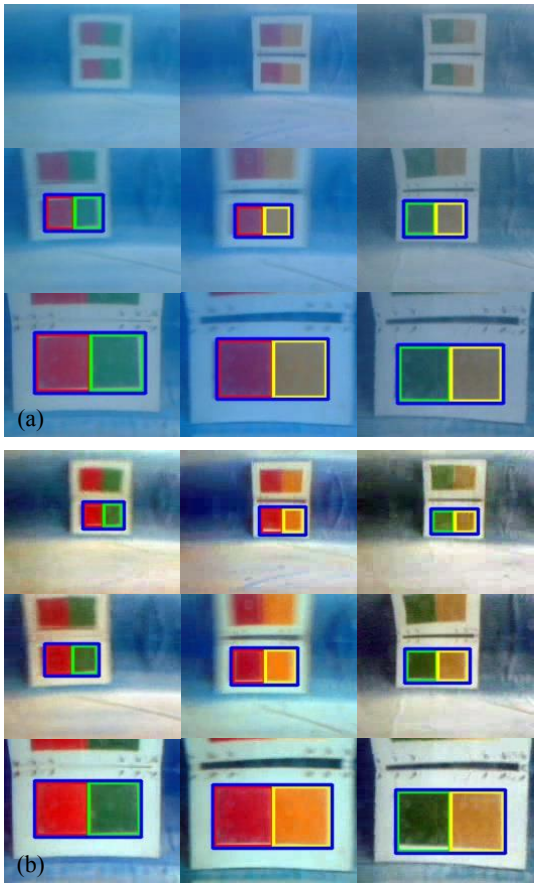

Fig. 9. The image precessing results without (a) and with AACE preprocessing (b), when robotic fish is swimming to various targets at different distances.

can make more comprehensive planning and response. At the middle distance (90 cm $\sim$ 120 cm), recognition ratios improve slightly by using AACE . Contrastively, the recognition ratios with AACE decrease a little at the near distance (60 cm $\sim$ 90 cm). This may be caused by the relative large changes in target colors at near distance by using AACE, which can be avoided by using more reasonable threshold value.

5.3 Distance Calculation Results

To smooth the calculated distance from Eqn. (6), Kalman filter is adopted. This section illustrates the features of the original

Table 1. Recognition ratio of algorithm with and without AACE (%).

Distance (cm)	RG	GR	RY	YR	GY	YG
120∼150	15.7	24.4	31.5	50	5.4	43.8
120∼150 (AACE)	83.3	44.9	51.9	77.3	83.9	80.2
90∼120	97.2	98.4	94.8	41.8	80.0	67.9
90∼120 (AACE)	95.5	99.1	97.0	75.3	90.9	80.4
60∼90	97.5	97.3	98.2	96.2	93.8	87.8
60∼90 (AACE)	92.9	97.2	97.3	95.3	89.4	88.6

and Kalman-filtered distances while the robot is operating. The experiment is performed as follow: in the beginning, the robot catches the vision of one effective target without moving at a distance of 140 cm; at $t = 12$ s, the robot swims toward to the target with the approximate speed of 8 cm/s. Fig. 10 shows the results of the calculated distances with and without Kalman filter. It is notable that the filtered distance is more stable and accurate compared with the real distance.

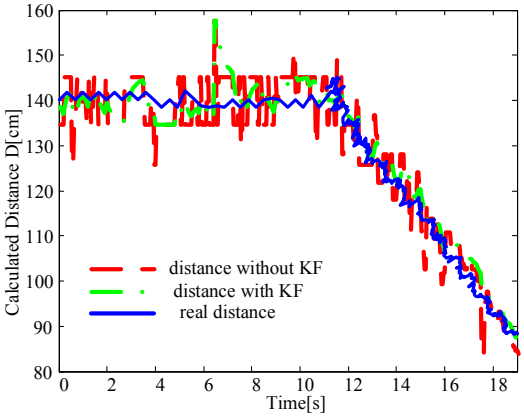

Fig. 10. The calculated distance processed with and without Kalman filter.

6. CONCLUSION AND FUTURE WORK

This paper proposes a novel adaptive and online underwater image processing approach implemented on a miniature robotic fish with low computational resources. To tackle the problem of nonuniform illumination, poor color contrast and motion blur in underwater image, an AACE model is performed to preprocess the obtained image, which greatly improves the image quality and benefits the subsequent image processing. After that, adaptive threshold segmentation, lump detection, reflection elimination are sequentially executed, and then, the targets are identified in a robust way while the robot is swimming. Finally, a Kalman-filtered distance between the robot and the target is calculated for further real-time applications.

The algorithm is performed online while the robotic fish is swimming in a tank with six artificial colored targets. The conducted results have demonstrated that the proposed underwater image processing algorithm is adaptive, efficient and low-computation, which makes it very suitable to practical applications of the miniature (bio-inspired) swimming robots with limited computational resources.

It is anticipated that the proposed underwater image processing algorithm will benefit practical applications of underwater robots, such as vision-based motion control and global localization. For these purposes, interesting topics like visual control system, multi-sensor localization system are worthy of further investigation.

REFERENCES

Artusi, A., Gatta, C., Marini, D., Purgathofer, W., and Rizzi, A. (2006). Speed-up technique for a local automatic colour equalization model. *Computer Graphics Forum*, 25(1), 5–14.

Bazeille, S., Quidu, I., Jaulin, L., Malkasse, J.P., and Others (2006). Automatic underwater image pre-processing. *Proceedings of CMM'06*.

Chambah, M., Semani, D., Renouf, A., Courtellemont, P., and Rizzi, A. (2003). Underwater color constancy: enhancement of automatic live fish recognition. In *Proc. SPIE*, volume 5293, 157–168.

CJ, P. and PU, P.K. (2011). An image based technique for enhancement of underwater images. *International Journal of Machine Intelligence*, 4(3), 217–224.

Feihu, S., Junzhi, Y., and Xu, D. (2013). Visual measurement and control for underwater robots: A survey. In *25th Chinese Control and Decision Conference (CCDC)*, 333–338.

Horgan, J. and Toal, D. (2006). Review of machine vision applications in unmanned underwater vehicles. In *9th International Conference on Control, Automation, Robotics and Vision, ICARCV '06*, 1–6.

Hu, Y., Zhao, W., Xie, G., and Wang, L. (2009). Development and target following of vision-based autonomous robotic fish. *Robotica*, 27(07), 1075–1089.

Iqbal, K., Abdul Salam, R., Osman, M., Talib, A.Z., and Others (2007). Underwater image enhancement using an integrated colour model. *IAENG International Journal of Computer Science*, 32(2), 239–244.

Lee, D., Kim, G., Kim, D., Myung, H., and Choi, H.T. (2012). Vision-based object detection and tracking for autonomous navigation of underwater robots. *Ocean Engineering*, 48, 59–68.

Mahiddine, A., Seinturier, J., Bo I, J.M., and Merad, P.D.D. (2012). Performances analysis of underwater image preprocessing techniques on the repeatability of sift and surf descriptors. In *WSCG 2012: 20th International Conference on Computer Graphics, Visualization and Computer Vision*.

Negre, A., Pradalier, C.E.D., and Dunbabin, M. (2008). Robust vision-based underwater target identification and homing using self-similar landmarks. 51–60.

Raimondo, S. and Silvia, C. (2010). Underwater image processing: state of the art of restoration and image enhancement methods. *EURASIP Journal on Advances in Signal Processing*. doi:10.1155/2010/746052.

Sehgal, A., Kadarusman, J., and Fife, L.D. (2004). Touch: A robotic vision system for underwater object tracking. In *IEEE Conference on Robotics, Automation And Mechatronics*, volume 1, 455–460.

Sural, S., Gang, Q., and Pramanik, S. (2002). Segmentation and histogram generation using the hsv color space for image retrieval. In *International Conference on Image Processing*, volume 2, 589–592.

Wang, W., Guo, J., Wang, Z., and Xie, G. (2013). Neural controller for swimming modes and gait transition on an ostraciiform fish robot. IEEE/ASME International Conference on Advanced Intelligent Mechatronics (AIM), 1564–1569.

Yu, S.C., Ura, T., Fujii, T., and Kondo, H. (2001). Navigation of autonomous underwater vehicles based on artificial underwater landmarks. In *MTS/IEEE Conference and Exhibition OCEANS*, volume 1, 409–416.